Cellulose
https://doi.org/10.1007/s10570-023-05368-5

ORIGINAL RESEARCH

Simple method for obtaining regenerated cellulose nanoparticles from delignified coffee parchment, and their use in fabricating blended films

Francisco Campuzano · Diana Marcela Escobar · Ana María Torres L

Received: 6 January 2023 / Accepted: 29 June 2023

Abstract Coffee parchment is one of the residues generated in coffee processing and has been poorly explored for value-added applications. It has been reported that coffee parchment has a high cellulose content (40–49%). Cellulose has been studied in many fields and specifically regenerated cellulose has been explored for many applications. Then, in this work a simple method for obtaining regenerated cellulose nanoparticles (RCNPs) from delignified coffee parchment, was determined. A complete physicochemical characterization of RCNPs obtained is presented, FTIR showed high cellulose purity, and XRD analysis showed high crystallinity of cellulose II. TEM images revealed that nanoparticles have spherical morphology. TGA showed good thermal stability and DLS allowed to determine the stability of suspension and the Z-average of the particles. The application of RCNPs on film formation was also evaluated when blended with PVA and Glycerol showing good mechanical properties with potential application on food packing.

F. Campuzano (✉)
Biomaterials Research Group, Faculty of Engineering, University of Antioquia, 19Th Avenue # 26Th - 24, La Ceja, Colombia
e-mail: fjose.campuzano@udea.edu.co

D. M. Escobar · A. M. Torres L
Biomaterials Research Group, Professor Faculty of Engineering, University of Antioquia, Medellín, Colombia

Keywords Regenerated cellulose nanoparticles · PVA · Blended films · Coffee parchment

Introduction

Coffee is one of the most consumed beverages in the world. Grain processing to get roasted coffee generates several residues, which can be processed by either the dry or wet method. In major coffee-producing countries such as Colombia, which annually produces approximately 750,000 tons of coffee beans (Federación Nacional de Cafeteros de Colombia 2021), the wet method is used and generates several residues throughout different processes. Specifically, during the dehulling process, a mechanical method is used to remove the outer layer of the dehusked coffee beans, known as coffee parchment (CP). About 39% of the coffee grains produced through this method consist of CP (Alves et al. 2017). Other by-products are generated in both processing methods, such as coffee husks, which are the red layer of the coffee berry, and the coffee silverskin, another inner layer of coffee beans. Additionally, obtaining the beverage generates spent coffee grounds. These other by-products have been widely explored for revalorization, such as obtaining nanocellulose, with good outcomes (Alghooneh et al. 2017; Dao et al. 2022; Zeleke et al. 2022; Shi et al. 2021; Kanai et al. 2020; Karunakaran et al. 2023). Nevertheless, CP is poorly utilized, and its main usages are focused on energy production or as livestock feed additives, which do not represent

Published online: 15 July 2023

value-added uses, evidencing a lack of revalorization of this by-product (Rodríguez Valencia and Zambrano Franco 2010; Franca et al. 2009; Limousy et al. 2017). On the other hand, it has been reported that CP has a high content of cellulose, ranging from 40 to 49% (Bekalo and Reinhardt 2010), which is interesting, since other coffee by-products have lower cellulose contents, ranging from 12 to 34% and have been successfully used for obtaining cellulose (Ballesteros et al. 2014; Karunakaran et al. 2023; Bekalo and Reinhardt 2010) making the CP a promising cellulose source.

Cellulose has been studied in many fields because of its properties. Specifically, regenerated cellulose (RC) or cellulose II has been studied for the fabricating of fibers, films, membranes, microspheres, hydrogels, and aerogels. RC fibers and films have been studied since many years ago, for example Viscose®, Tencel®, and cuprammonium rayon for the manufacturing of fabrics (S. Wang, Lu, and Zhang 2016), and cellophane and cuprophane for food packing with high mechanical properties (Klemm et al. 2005; Fink et al. 2001). Likewise, other methodologies for RC film fabrication has been studied for food packing purposes with high transparency, antimicrobial activity and pH responsive properties (Huang and Wang 2022; Xiong et al. 2010). Hydrogels have also been studied and show high stability, solvent resistance, and high compressive strength, as well as excellent biocompatibility, exhibiting potential application to be used as biomaterial (He et al. 2014). On the other hand, RC microspheres and aerogel beads have been demonstrated usability on separation applications like chromatography, and biocatalyst immobilization and carriers (Tu et al. 2021; Druel et al. 2020). Additionally, RC has been widely employed in blended materials with synergistic effects in their properties (Tu et al. 2021).

Moreover, regenerated cellulose nanoparticles (RCNPs) can be obtained through solubilizing cellulose in sodium hydroxide/urea solutions at low temperatures or in deep eutectic solvents, followed by regeneration on deionized water, ethanol or sulfuric acid solutions, to form a RC hydrogel. Then, using mechanical methods such as ultrasonication, microfluidization, melt extrusion or rotative homogenizers, RCNPs can be obtained (Choi et al. 2019; Shin et al. 2018; Zhang et al. 2016; Adsul et al. 2012; Han and Seo 2021; Sirviö 2019). However, these methods are time-consuming.

The aim of this work was to obtain RCNPs from a poorly explored source, coffee parchment, in order to revalorize this coffee by-product through a novel and facile approach, and to evaluate its potential use for film fabrication. A complete characterization of the RCNPs is presented, as well as an evaluation of the mechanical properties of the resulting films.

Materials and methods

Sample source and materials

CP was obtained from A. Laumayer y Compañía Exportadores de Café S.A.S. This sample came from the processing of the species *Coffea arabica* variety Castillo®, from the department of Antioquia (Colombia). The sample was sieved and a portion of the material with a mean diameter of 1.3 mm was separated for delignification process. All reagents used were analytical grade and the Polyvinyl alcohol (PVA) used had a molecular weight between 89 and 98 kDa.

Production of regenerated cellulose nanoparticles

Coffee parchment delignification

Samples were washed with ethanol 95% v/v at boiling point for 15 min in a 1:10 ratio (g:mL) with frequent stirring with a glass rod. The mixture was allowed to cool and was decanted, and then the extracted CP was dried at 50 °C for 24 h. After this, 5 g of extracted CP were mixed with 50 mL of sodium hydroxide 2.4%w/v, then 25 mL of hydrogen peroxide 20%v/v were slowly dropped, and the mixture was kept for 4 h with constant stirring at 50 °C. Then, the samples were decanted, and the process described above was made a second time. Subsequently, samples were decanted and washed with distilled water. The bleached samples were dried at 50 °C for 24 h.

A bleaching refinement was carried out. In brief, the bleached samples were grounded with a POLY-MIX® knife mill to a particle size less than 1000 µm. Then 10 g of bleached CP were treated with 100 mL of sodium hypochlorite 3.3% w/v at pH between 8

and 9, with vigorous stirring for 3 h at 50 °C. Afterwards, the solids were separated with centrifuging at 5000 rpm for 10 min. The remaining solids were treated again with sodium hypochlorite in the same conditions above described. The treated material was washed with distilled water by centrifuging at 5000 rpm for 10 min several times, until achieving a conductivity less than 50 µS/cm to obtain a cellulose pulp.

The above experimental conditions were previously established in our laboratory.

Solubilization and regeneration of cellulose

Cellulose pulp solubilization was carried out according to a methodology widely reported (Nomura et al. 2020; Adsul et al. 2012). In brief, a sodium hydroxide/urea aqueous solution was prepared. 14 g of sodium hydroxide and 24 g of urea were solubilized in 162 g of distilled water and then pre-cooled to -15 °C. Then, 60 g of cellulose pulp was added and mechanically stirred at 2400 rpm for 10 min into an ice bath. Afterwards, the mixture was centrifuged at 1700 g for 10 min to separate the non-solubilized cellulose.

The cellulose solution was regenerated into cellulose nanoparticles as schematized in Fig. 1. The cellulose solution was subjected to mechanical stirring at 1400 rpm, while a regenerating solution was slowly dropped until the cellulose was regenerated. The regenerating solution contained sodium sulfate 3.3%w/v and 3.3%v/v sulfuric acid. The RCNPs suspension was centrifuged at 5000 rpm for 10 min and cellulose was resuspended in distilled water and taken to dialysis into cellulose membranes. Water changes were carried out until the conductivity of

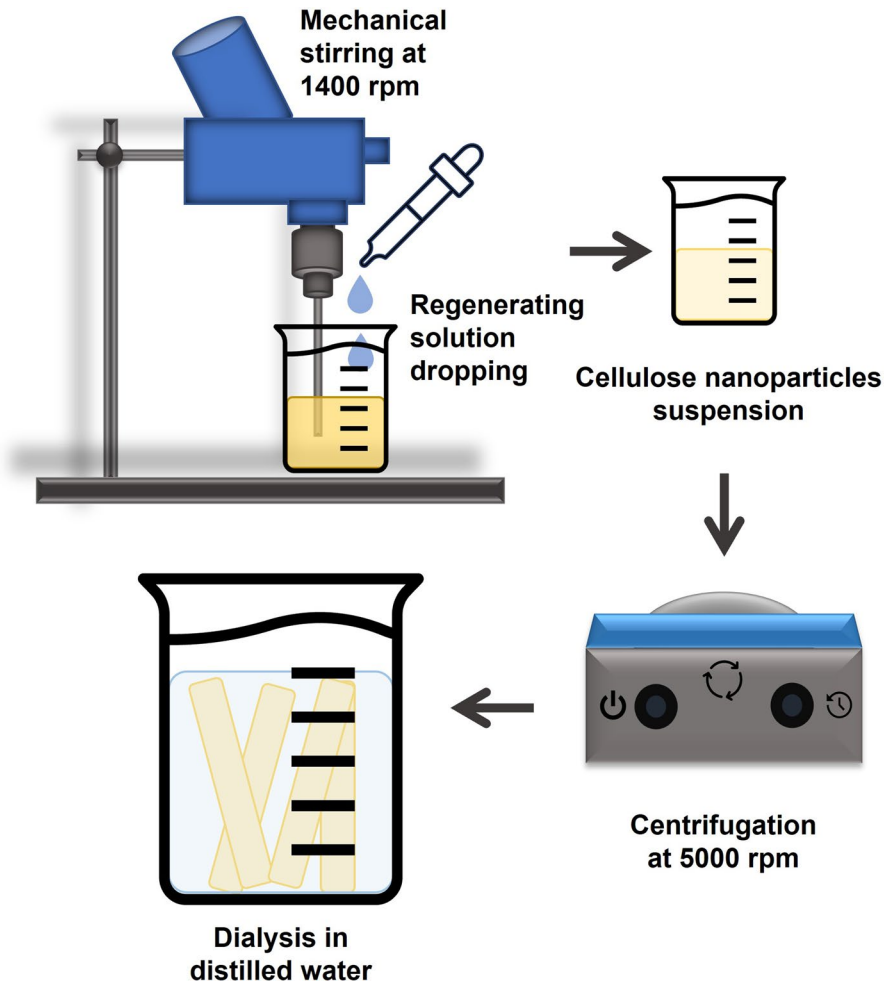

Fig. 1 Cellulose regeneration scheme

cellulose suspension was less than 50 µS/cm. The process was made by triplicate.

RCNPs production yield

The yield was determined by gravimetric analysis. The measurement was performed at each stage of the process by triplicate, and the Eq. (1) was used.

$$Y\left(g_{product}/100g_{input}\right) = \frac{Input\ mass}{product\ mass} \times 100 \quad (1)$$

where Y is the efficiency in grams of product per 100 g of input in each process, input mass is the mass of the material entering the process on a moisture-free basis, and product mass is the mass of the material resulting from the process on a moisture-free basis. To achieve the measurement on a moisture-free basis, the samples were dried for 24 h at 105 °C in previously dried and weighed glass containers, and then allowed to cool completely into a desiccator for 1 h before being weighed.

Characterization

Infrared spectroscopy

Cellulose suspension was freeze-dried, and a Fourier Transform Infrared Spectroscopy (FTIR) was carried out from 400 to 4000 cm^{-1} in a Spectrum Two of the Perkin Elmer brand. Data were processed and plotted with Matplotlib on Python.

Morphology analysis

Samples were stained with uranyl acetate and dried on a carbon membrane and analyzed with Transmission Electron Microscopy (TEM). The assay was carried out with a microscope FEI Tecnai F20 Super Twin TMP.

Crystallinity analysis

The crystallinity of RCNPs was analyzed using X-Ray Diffraction (XRD). Cellulose suspension was freeze-dried to obtain a powder, which was then analyzed with a Malvern-PANalytical Empyrean 2012 in reflection mode. The analysis was conducted using a pixel detector 3D, a Cu source with $\lambda = 1.541874$ Å, a voltage of 45 kV, a current of 40 mA, and a step size of 0.013°. A sample holder of silicon crystal was used, and a blank run was captured. The data from the blank run were subtracted from that of the sample run to eliminate environmental noise contribution. The data were plotted using Matplotlib in Python.

Thermal profile determination

Cellulose suspension was freeze-dried, and the powder was subjected to a thermogravimetric analysis (TGA) in a TGA Q500 TA Instruments. Sample was heated from room temperature to 600 °C at a rate of 10 °C min^{-1} under a flow of nitrogen. Data were processed and plotted with Matplotlib on Python. In addition, the differential thermogravimetric (DTG) curve was determined.

Dynamic light scattering (DLS) and Z potential

The cellulose suspension was diluted until 0.1 mg/mL and sonicated, then the samples were analyzed on a Malvern-PANalytical Zetasizer Nano. Size and Z potential were determined. For size measurement polyethylene glycol 3350 3%w/v was added to the suspension as dispersant. The measurements were made by triplicate.

Film preparation and mechanical properties evaluation

RCNPs/PVA/Glycerol blended films

A mixture of RCNPs/PVA/Glycerol was made in a 50:25:25 ratio on a dry basis. For this, 0.5 g of PVA and 0.5 g of glycerol were added to 50 mL of RCNPs suspension 2% w/v. The blend was stirred for 5 min, then it was taken into an ultrasonic bath for 10 min. Afterwards, the blend was stirred at 85 °C for 20 min. Finally, 10 mL of mixture was poured on rectangular silicone molds of 8 cm length and 5.5 cm width, to obtain five films, and were let dry for 48 h at room temperature. The process was made by triplicate.

PVA/glycerol blended films

PVA/Glycerol blended films were fabricated as controls, for this a solution of PVA/Glycerol was made in a 50:50 ratio, for which 1 g of PVA and 1 g of glycerol

were added to 50 mL of water and stirred at 85 °C for 20 min, then the solution was poured on rectangular silicone molds of 8 cm length and 5.5 cm width, 10 mL in each mold. The films were let dry for 48 h at room temperature. The process was made by triplicate.

Mechanical properties of films

A tensile testing was carried out to the films according to the ASTM D882-12 with some modifications (ASTM 2017). The test specimens were cut in strips of 67 mm length and 10 mm width, avoiding nicks and tears that could cause premature failures. The testing was carried out using a universal testing machine Digimess with self-tightening roller grips at a speed of 5 mm min^{-1}. The testing was made twice for each film.

Results and discussion

The Fig. 2 shows both a concentrated and a diluted suspension of the RCNPs, that were characterized to determine its physicochemical properties.

Infrared spectroscopy

The FTIR spectrum of RCNPs is shown in Fig. 3, and the main bands of cellulose are presented. The broad band in 3325 cm^{-1} is associated with the hydrogen bonds between RC chains, which suggests that, after regeneration, cellulose rearranges into an organize structure maintained with these bonds (Coelho de Carvalho Benini et al. 2017; Lim et al. 2020; Kale et al. 2020; Najeeb et al. 2021). The band in 2890 cm^{-1} has been related with the stretching movements in C–H bonds of methylene groups of cellulose (Coelho de Carvalho Benini et al. 2017; Lim et al. 2020; Kale et al. 2020; Najeeb et al. 2021; Rizwan et al. 2021). There is a band around 1624 cm^{-1} related with the bending movement of O–H bond in water, which suggests water trapping into RC chains. It has also been related with the same movement of O–H in cellulose (Jyothibasu et al. 2019; Pang et al. 2014; Mohamed et al. 2016; Kilulya et al. 2011). Some bands have been associated with crystalline organization on cellulose by hydrogen bonding, in this case, there are such two bands in 1420 cm^{-1} and 1378 cm^{-1} (Coelho de Carvalho Benini et al. 2017; Choi et al.

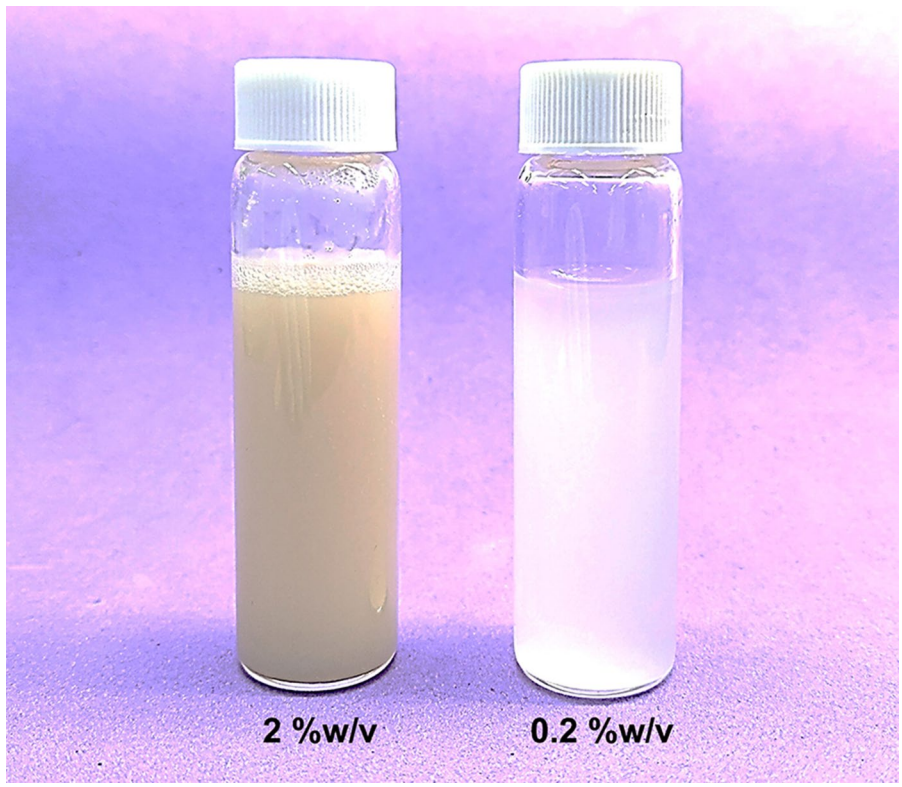

Fig. 2 RCNPs suspension obtained

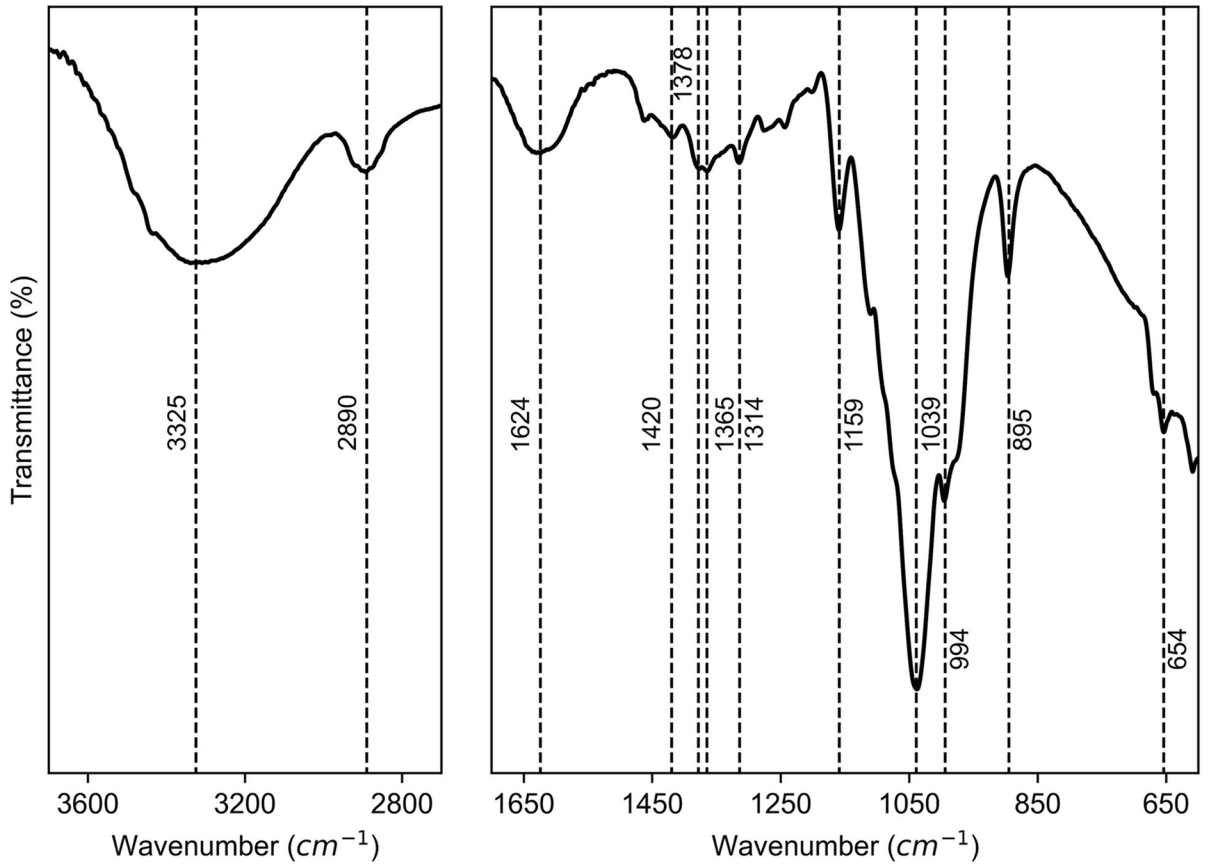

Fig. 3 FTIR spectrum of RCNPs. Main bands are marked with dotted lines

2019). Stretching movements of some C–H bonds in cellulose can show a band in 1365 cm^{-1}, as well as the 1314 cm^{-1} band can be associated with coupled wagging movements between C–H and primary alcohols in cellulose (Silverstein et al. 2005; Choi et al. 2019). The asymmetric stretching of C–O–C bonds in the glucose ring generates a band in 1159 cm^{-1} (Silverstein et al. 2005). The main band of cellulose is presented in 1039 cm^{-1} and is attributed to the overlapping of the band of the cyclic ether on glucose and the band of C–O bonds in alcohols of glucose (Coelho de Carvalho Benini et al. 2017; Lim et al. 2020; Kale et al. 2020; Najeeb et al. 2021; Silverstein et al. 2005). There are also bands associated with amorphous regions in cellulose, in this case, there are such two bands in 994 cm^{-1} and 654 cm^{-1} (Coelho de Carvalho Benini et al. 2017; Choi et al. 2019). Finally, the band in 895 cm^{-1} corresponds to β-(1–4) glycosidic bonds of cellulose (Coelho de Carvalho Benini et al. 2017; Lim et al. 2020; Kale et al. 2020).

The crystallinity of cellulose has been determined from the absorbance ratio of bands associated with crystalline and amorphous regions, using Eq. (2) (Coelho de Carvalho Benini et al. 2017; Choi et al. 2019; Adsul et al. 2012).

$$I_c = \frac{A_c}{A_a} x100\% \tag{2}$$

where I_c is the crystallinity index, A_c is the absorbance of the crystalline band, and A_a is the absorbance of the amorphous band.

Specifically, a ratio between the 1372/654 and 1420/895 bands has been reported (Coelho de Carvalho Benini et al. 2017; Choi et al. 2019; Adsul et al. 2012). In this study, for similar values, a crystallinity of 35% with the first ratio, and 47% with the second

are obtained. Although these values are not consistent with each other, it can be stated that the regeneration methodology employed gives rise to crystalline regions. This is a positive result due to the benefits that have been attributed to crystalline cellulose (George and Sabapathi 2015; Abdul Khalil et al. 2015; Debnath et al. 2021; Seidi et al. 2022; Wang et al. 2022).

In short, this result allows determining that the RC obtained presents high purity, since no bands were found that could be associated to other compounds, in addition, it was possible to determine that the methodology used gives rise to regenerated cellulose with crystalline regions.

Crystallinity analysis

Figure 4 shows the X-ray diffractogram of regenerated cellulose. The three main diffraction peaks are presented at 12.2°, 20.1° and 21.6°. Monoclinic models have been proposed for the crystal system presented in cellulose II, and different techniques have been applied to determine the lattice parameters that have been used to simulate the X-ray diffraction patterns, which are consistent with the pattern shown in Fig. 4 (Nam et al. 2016; French and Santiago Cintrón 2013; French 2014). Likewise, the diffraction patterns for RC have been experimentally determined where the marked peaks in Fig. 4 are reported (Nomura et al. 2020; Azubuike et al. 2012; Han and Seo 2021; Jyothibasu et al. 2019; Shin et al. 2018; Sirviö 2019).

The crystallinity of this type of cellulose can also be estimated with the Segal method using the Eq. (3) (Segal et al. 1959).

$$I_c = \frac{I_{(200)} - I_{am}}{I_{(200)}} x100\% \quad (3)$$

where, I_c is the crystallinity index, $I_{(200)}$ is the intensity of diffraction of plane (200) and I_{am} is the intensity of amorphous phase at around 18°. For regenerated cellulose it has been reported the use of the intensity of the diffraction peak of the (020) plane and an intensity of amorphous phase at 16° (Nomura et al. 2020; Azubuike et al. 2012; Han and Seo 2021).

In this case, the crystallinity is around 75%, which is higher than that estimated through the band ratio of the infrared spectrum and other reported values (Nomura et al. 2020; Nam et al. 2016; Wang et al. 2022). Nevertheless, this technique has been criticized because it can underestimate the amorphous content (Nam et al. 2016). However, it continues to be widely used to estimate the crystallinity of cellulose, and the obtained result is very favorable. It indicates that the regeneration methodology used allowed for the rearrangement of the cellulose chains in a way that highly favored the formation of crystals.

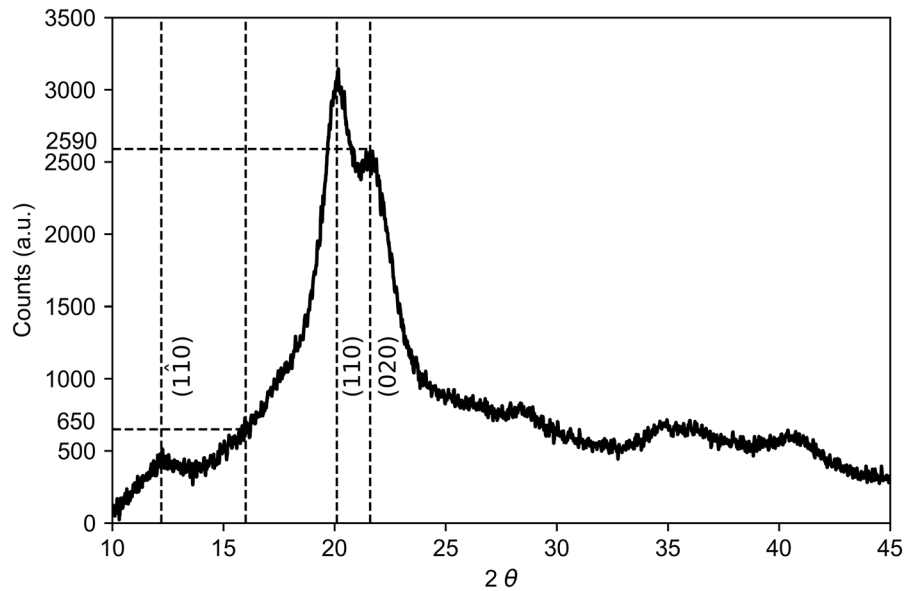

Fig. 4 XRD pattern of regenerated cellulose, main diffraction peaks are marked with respective planes

Morphology analysis

TEM images allow to determine that the cellulose obtained was within the nanometric scale, with an average diameter of 32.8 ± 9.3 nm. This value was calculated after measuring 40 particles in several images. Figure 5 shows that the morphology of the particles obtained is spherical, and that they tend to agglomerate but present a very homogeneous size distribution. Agglomeration may be favorable since interactions between the nanoparticles are required to generate a macroscopic structure with appropriate mechanical properties. Considering that cellulose has many OH groups, hydrogen bonding could be the responsible for agglomeration.

A concentric layered morphology was also observed (Fig. 6), which could be cellulose nano-onions due to their similarity to carbon nano-onions (Adhikari et al. 2019). It is possible that the regeneration methodology had led to a layered growth of the particles, which give rise to this morphology. This result has not been reported previously and could be of interest for applications such as encapsulation of molecules between the cellulose layers, or for coating other particles, obtaining Core–Shell nanostructures. However, it is necessary to study the conditions that

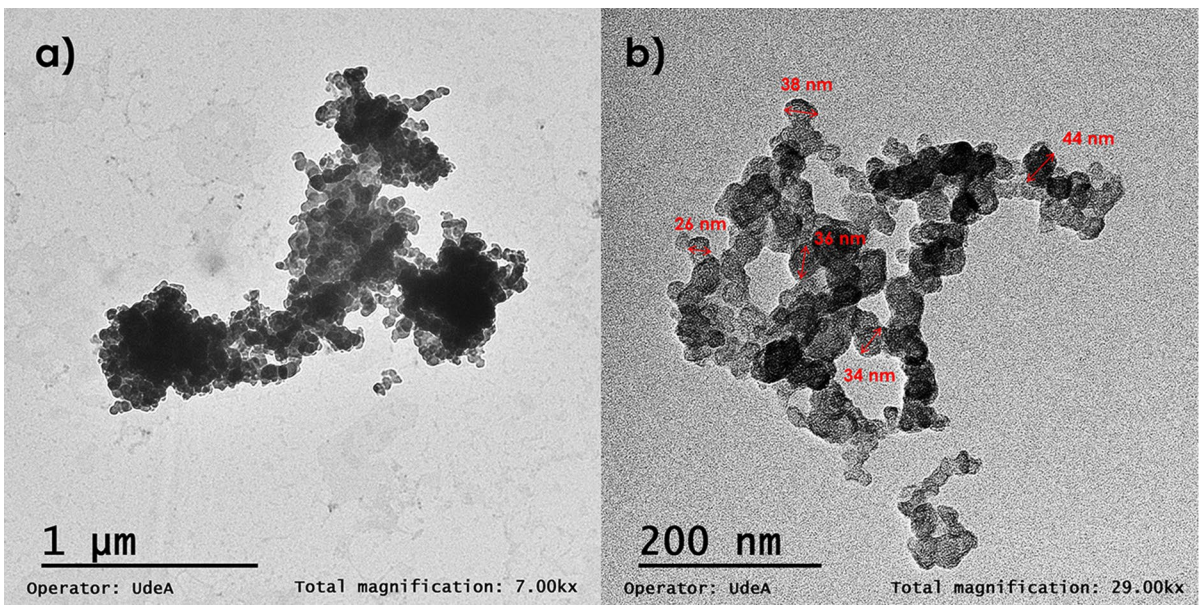

Fig. 5 TEM images of RCNPs at different magnifications as indicated on each image. Some particles diameters are presented in (**b**)

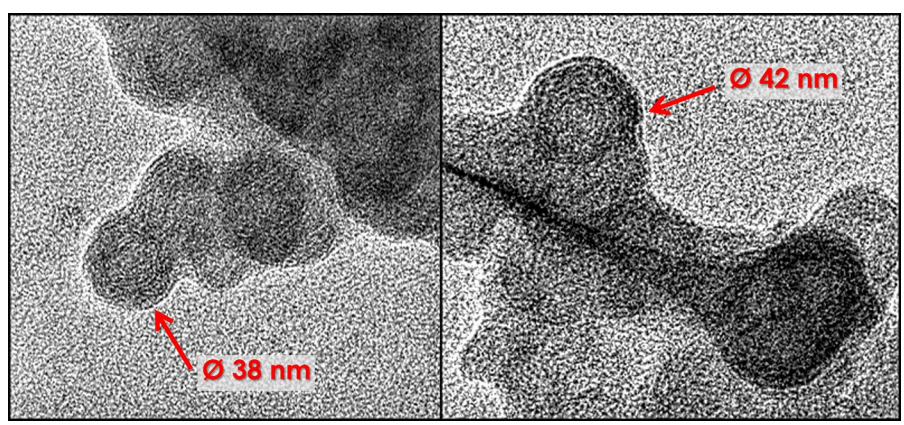

Fig. 6 TEM images of RCNPs with concentric layered morphology. Annotations with the diameters are presented

favor the formation of these nanostructures, since they were not observed in all cases.

Thermal profile determination

The thermal degradation profile of the RCNPs was obtained and is shown in Fig. 7. From the TGA curve, the derivative (DTG) was calculated to identify the different stages. The first stage, from room temperature to 150 °C, corresponds to the evaporation of water and has a maximum evaporation rate at 75 °C, the percentage of humidity was 3.5%. The degradation of the material begins at 150 °C, with a second stage occurring between this temperature and 313 °C with a maximum degradation rate at 288 °C, and with a mass loss percentage of 42%. Then a mass loss occurs up to 600 °C with a maximum degradation at 333 °C, in which there is a loss of 33% of the mass. The remaining mass is 21.5% and may correspond to cellulose pyrolysis products since the test is performed in a non-oxidizing atmosphere.

Considering that the analysis of the infrared spectrum of cellulose did not show the presence of impurities of other materials, then, the two degradation stages observed in Fig. 7 should correspond to cellulose degradation and could be explained from the crystallinity point of view. It is possible that in the regeneration methodology, particles with a higher crystallinity than others are obtained, giving rise to the presence of one material more thermically stable than another. In that case, 44% of the cellulose in the material would have high crystallinity and 66% low or no crystallinity, which is consistent with crystallinity obtained by FTIR and then also supports crystalline cellulose regeneration. A decrease in the maximum degradation temperature for a completely amorphous cellulose has been observed, which is consistent with the hypothesis stated here (Hu et al. 2018). Likewise, similar thermal behavior to that obtained here has been attributed to amorphous cellulose (Kumar et al. 2020).

DLS and Z potential

Even though the samples were conditioned with sonication to disaggregate the particles, the DLS showed a Z average of 403.3 ± 51.6 nm, which according to TEM images, would correspond to the size of the agglomerations. This suggests that the interaction of the particles is quite strong, and that polyethylene glycol might not be the best dispersant in this case. Furthermore, the agglomerations have a closed distribution with a polydispersity index of 0.38 ± 0.02.

On the other hand, the Z potential of the particles is -26.46 ± 0.28 mV, suggesting some instability of suspension, which explains aggregation of the particles, which was already observed in the TEM images and corroborated by DLS. For suspension applications of nano-cellulose it would be of interest to study how to modify this potential to keep the particles

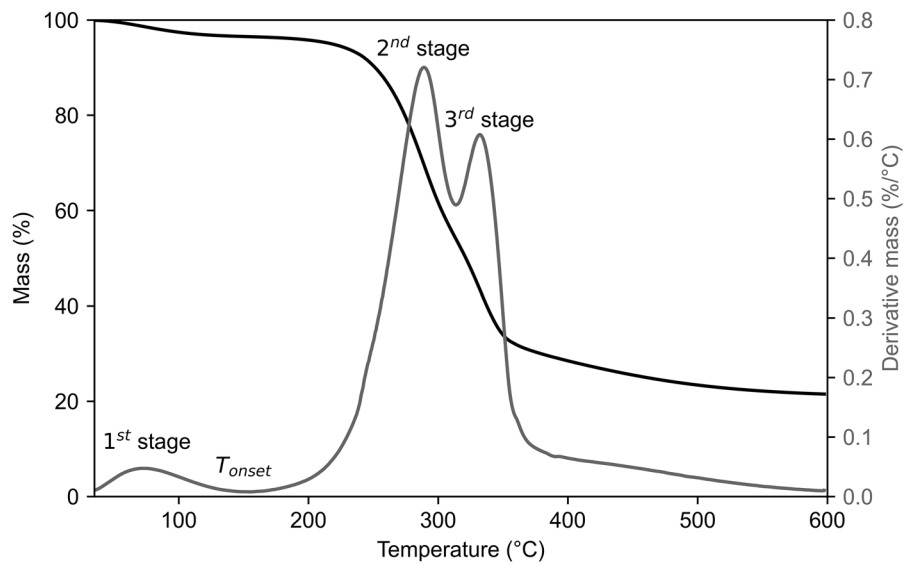

Fig. 7 TGA (black) and DTG (gray) of regenerated cellulose. Different stages of thermal degradation are marked

stable for a longer time, however, this is beyond the scope of this work.

RCNPs production yield

Table 1 shows the yield of each stage of the process, as well as the yield of the whole process.

The solubilization and regeneration stage is the least efficient, achieving the solubilization of 30.00% of the cellulose pulp. However, it was observed that the solid material that remains non-solubilized contains a significant amount of unregenerate cellulose, which can be recovered by washing with distilled water and then regenerated. On the other hand, this remaining solid material can be subjected to a second solubilization cycle in which a cellulose solution is obtained again. Thus, it would be interesting to make a cost–benefit analysis of performing multiple solubilization cycles, as well as to evaluate the properties of the unregenerated cellulose remaining in the solid material after centrifuging.

Mechanical properties of films

Previous experimentations showed that RCNPs cannot form films due to its high stiffness, then the film formation was evaluated when blended with PVA and Glycerol to provide elasticity and plasticity, respectively.

Then the Young's modulus, tensile strength and elongation at break were determined for RCNPs/PVA/Glycerol and PVA/Glycerol blended films and they are presented in Fig. 8. It is noted that RCNPs caused an evident increment on stiffness by obtaining a Young's Modulus 450% higher compared to control. The tensile strength is also significantly higher in blended films with RCNPs, obtaining an increment of 46%. Nevertheless, the elongation at break is diminished in 85% by the addition of RCNPs.

There are some reports of RC/PVA blended films with tensile strengths between 60 and 80 MPa, and Young's Modulus of 3 GPa without glycerol (Zhang et al. 2012; Zhu et al. 2020). However, the addition of Glycerol has been reported as plasticizer, which can explain the mechanical properties obtained (Setiawan et al. 2022; Abd Karim et al. 2022; Abdullah et al. 2022). Additionally, PVA presents a wide range of properties according to its molecular weight and hydrolyzation grade, which also explains the differences obtained (Alipoori et al. 2021; Fu et al. 2022).

This result can also be related with crystallinity and interparticle interactions. The RCNPs obtained have a high crystallinity compared with many other RC reported in literature (Nomura et al. 2020; Azubuike et al. 2012; Han and Seo 2021; Jyothibasu et al. 2019; Shin et al. 2018; Sirviö 2019). High crystallinity indexes in cellulose have been related with higher mechanical properties (George and Sabapathi 2015; Abdul Khalil et al. 2015; Mokhena et al. 2021; Seidi et al. 2022), then RCNPs in blended films can cause an increase in mechanical properties compared with control. Moreover, as observed in TEM images and Z potential measurements, the particles tend to agglomerate, probably by mean of hydrogen bonding. Glycerol and PVA are rich in OH groups that can interact with those present on RCNPs generating a physical cross-linking that can cause the mechanical properties to increase. Similarly, the decrease of elongation capacity is an expected effect because cellulose is not as elastic as PVA (Alipoori et al. 2021; Fu et al. 2022; Seidi et al. 2022; Mokhena et al. 2021).

Biopolymers for food packing applications have been reported with similar mechanical properties to those obtain in the RCNPs/PVA/Glycerol blended films. Tensile strength has been reported between 3.4 and 10.32 MPa, Young's modulus between 63 and 177 MPa and Elongation at break between 3.1 and

Table 1 Yields achieved in each process for the production of RCNPs

Process	Input	Product	$Y\left(\frac{g_{product}}{100g_{input}}\right)$
Hydrogen peroxide bleaching	Coffee parchment washed with ethanol	Bleached coffee parchment	85.28 ± 0.87
Bleaching refinement	Bleached coffee parchment	Cellulose pulp	80.94 ± 0.54
Solubilization/regeneration	Cellulose pulp	RCNPs	30.00 ± 0.01
Whole process	Coffee parchment washed with ethanol	RCNPs	20.67 ± 0.68

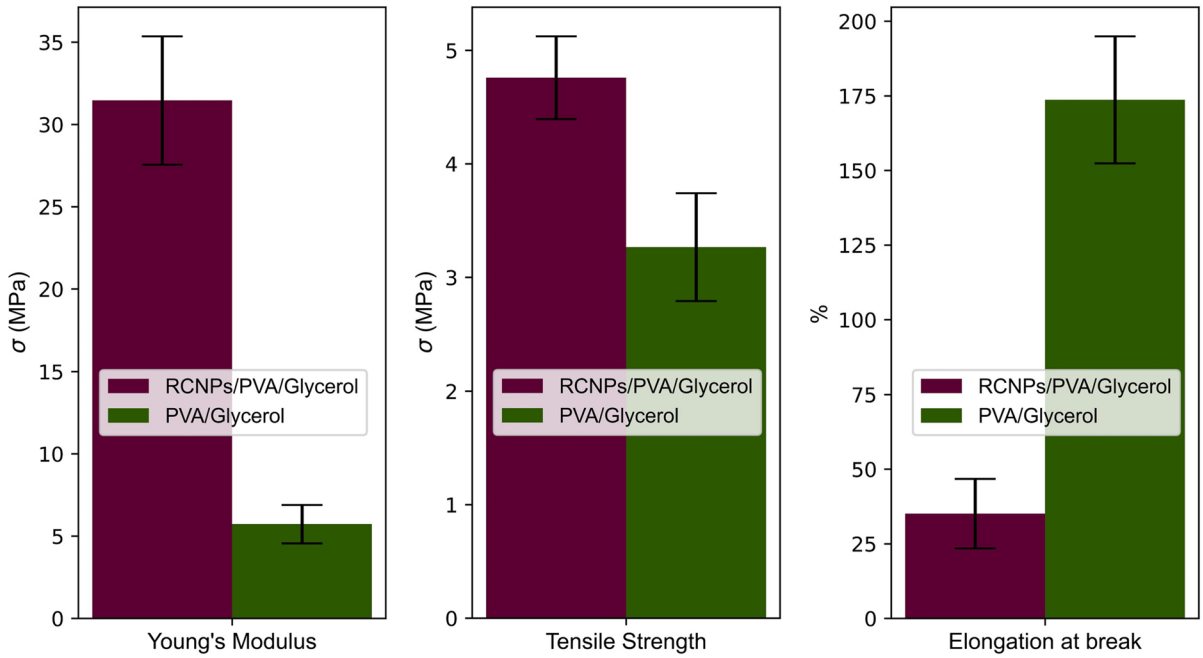

Fig. 8 Mechanical properties obtained for PVA/Glycerol and RCNPs/PVA/Glycerol blended films

179% (Jafarzadeh et al. 2017; Hassannia-Kolaee et al. 2016; Hashemi Tabatabaei et al. 2018; Hasheminya et al. 2018; Pagno et al. 2015). Considering that cellulose and PVA have been used for food packing applications (Cazón et al. 2019; Huang and Wang 2022), this could be a possible application for the blended films here obtained.

Conclusions

The cellulose pulp obtained was solubilized by 30.00% using the described methodology. The proposed regeneration method allowed regenerating the solubilized cellulose into spherical nanoparticles as seen in TEM images, but they tend to agglomerate due to a low Z potential. The FTIR results indicate a high purity of the cellulose and allowed determining that the crystallinity of the material is between 35 and 47%. XRD confirmed the presence of cellulose II crystals with a crystallinity of 75% calculated by Segal's method, which is still the more accepted method, then the RCNPs obtained have a high crystallinity. TGA shows a good thermal stability and suggests crystalline and amorphous coexistent domains in RCNPS.

The whole process to obtain RCNPs has a yield of 20.67 ± 0.68 g of RCNPs per 100 g of washed coffee parchment, which is a satisfactory yield, considering that only around a half of coffee parchment is cellulose.

On the other hand, the RCNPs obtained can be used to form flexible films with good mechanical properties when blended with PVA and Glycerol, that could be used for food packing applications.

Acknowledgments The authors thank Biomaterials Research Group from the University of Antioquia for the support given. This work was financed by Biomaterials Research Group from the University of Antioquia

Author contributions FC: methodology, validation, investigation, and writing—original draft. DME: project administration, conceptualization, and writing—review & editing. AMTL: conceptualization, and writing—review & editing.

Funding Open Access funding provided by Colombia Consortium. The authors declare that no funds, grants, or other support were received during the preparation of this manuscript.

Availability of data and materials Not applicable.

Declarations

Conflict of interest The authors have no relevant financial or non-financial interests to disclose.

Ethics approval and consent to participate Not applicable.

Consent for publication Not applicable.

References

Abd Karim SF, Jai J, Ku Hamid KH, Abdol Aziz RA, Ab Rahim MAS, Bin Rosley MF (2022) Characterization of glycerol and aloe vera as plasticizer in polyethylene/starch-based film. Pertanika J Sci Technol 30(2):1527–1544. https://doi.org/10.47836/pjst.30.2.37

Abdul Khalil HPS, Bhat AH, Abu Bakar A, Tahir PM, Zaidul ISM, Jawaid M (2015) Cellulosic nanocomposites from natural fibers for medical applications: a review. In: Handbook of polymer nanocomposites. Processing, performance and application, pp 475–511. Springer, Berlin. https://doi.org/10.1007/978-3-642-45232-1_72

Abdullah AM, Aziz SB, Brza MA, Saeed SR, Al-Asbahi BA, Sadiq NM, Ahmed AAA, Murad AR (2022) Glycerol as an efficient plasticizer to increase the DC conductivity and improve the ion transport parameters in biopolymer based electrolytes: XRD, FTIR and EIS studies. Arab J Chem 15(6):1037–1091. https://doi.org/10.1016/j.arabjc.2022.103791

Adhikari J, Keasberry NA, Mahadi AH, Yoshikawa H, Tamiya E, Ahmed MU (2019) An ultra-sensitive label-free electrochemiluminescence CKMB immunosensor using a novel nanocomposite-modified printed electrode. RSC Adv 9(59):34283–34292. https://doi.org/10.1039/c9ra05016g

Adsul M, Soni SK, Bhargava SK, Bansal V (2012) Facile approach for the dispersion of regenerated cellulose in aqueous system in the form of nanoparticles. Biomacromol 13(9):2890–2895. https://doi.org/10.1021/bm3009022

Alghooneh A, Amini AM, Behrouzian F, Razavi SMA (2017) Characterisation of cellulose from coffee silverskin. Int J Food Prop 20(11):2830–2843. https://doi.org/10.1080/10942912.2016.1253097

Alipoori S, Torkzadeh MM, Mazinani S, Aboutalebi SH, Sharif F (2021) Performance-tuning of PVA-based gel electrolytes by acid/PVA ratio and PVA molecular weight. SN Appl Sci 3(3):1–13. https://doi.org/10.1007/s42452-021-04182-7

Alves RC, Rodrigues F, Nunes MA, Vinha AF, Beatriz M, Oliveira PP (2017) State of the art in coffee processing by-products. In: Handbook of coffee processing by-products: sustainable applications, First, 1–26. Elsevier Inc. https://doi.org/10.1016/B978-0-12-811290-8.00001-3.

ASTM (2017) Standar test method for tensil properties of thin plastic sheeting. ASTM D882-12, issued 2017.

Azubuike CP, Rodríguez H, Okhamafe AO, Rogers RD (2012) Physicochemical properties of maize cob cellulose powders reconstituted from ionic liquid solution. Cellulose 19(2):425–433. https://doi.org/10.1007/s10570-011-9631-y

Ballesteros LF, Teixeira JA, Mussatto SI (2014) Chemical, functional, and structural properties of spent coffee grounds and coffee silverskin. Food Bioprocess Technol 7(12):3493–3503. https://doi.org/10.1007/s11947-014-1349-z

Bekalo SA, Reinhardt H-W (2010) Fibers of coffee husk and hulls for the production of particleboard. Mater Struct 43(8):1049–1060. https://doi.org/10.1617/s11527-009-9565-0

Cazón P, Velazquez G, Vázquez M (2019) Novel composite films from regenerated cellulose-glycerol-polyvinyl alcohol: mechanical and barrier properties. Food Hydrocolloids 89(April):481–491. https://doi.org/10.1016/j.foodhyd.2018.11.012

Choi SM, Lee MW, Shin EJ (2019) One-pot processing of regenerated cellulose nanoparticles/waterborne polyurethane nanocomposite for eco-friendly polyurethane matrix. Polymers 11(2):356. https://doi.org/10.3390/POLYM11020356

de Carvalho C, Benini KC, Voorwald HJC, Cioffi MOH, Milanese AC, Ornaghi HL (2017) Characterization of a new lignocellulosic fiber from Brazil: imperata brasiliensis (Brazilian Satintail) as an alternative source for nanocellulose extraction. J Nat Fibers 14(1):112–125. https://doi.org/10.1080/15440478.2016.1167647

Dao DN, Le PH, Do DX, Dang TMQ, Nguyen SK, Nguyen V (2022) Pectin and cellulose extracted from coffee pulps and their potential in formulating biopolymer films. Biomass Convers Bioref. https://doi.org/10.1007/s13399-022-02339-x

Debnath B, Haldar D, Purkait MK (2021) A critical review on the techniques used for the synthesis and applications of crystalline cellulose derived from agricultural wastes and forest residues. Carbohydr Polym 273(December):118537. https://doi.org/10.1016/j.carbpol.2021.118537

Druel L, Kenkel A, Baudron V, Buwalda S, Budtova T (2020) Cellulose aerogel microparticles via emulsion-coagulation technique. Biomacromol 21(5):1824–1831. https://doi.org/10.1021/acs.biomac.9b01725

Federación Nacional de Cafeteros de Colombia (2021) Informe de Gestión 2021. Informe de Gestión. https://doi.org/10.38141/10793.

Fink HP, Weigel P, Purz HJ, Ganster J (2001) Structure formation of regenerated cellulose materials from NMMO-solutions. Prog Polym Sci (oxford) 26(9):1473–1524. https://doi.org/10.1016/S0079-6700(01)00025-9

Franca A, Oliveira L, Franca AS (2009) Coffee processing solid wastes: current uses and future perspectives, agricultural wastes. Nova Publishers, New York

French AD (2014) Idealized powder diffraction patterns for cellulose polymorphs. Cellulose 21(2):885–896. https://doi.org/10.1007/s10570-013-0030-4

French AD, Cintrón MS (2013) Cellulose polymorphy, crystallite size, and the segal crystallinity index. Cellulose 20(1):583–588. https://doi.org/10.1007/s10570-012-9833-y

Fu ZZ, Guo SJ, Li CX, Wang Ke, Zhang Q, Qiang Fu (2022) Hydrogen-bond-dominated mechanical stretchability in PVA films: from phenomenological to numerical insights. Phys Chem Chem Phys 24(3):1885–1895. https://doi.org/10.1039/d1cp03893a

George J, Sabapathi SN (2015) Cellulose nanocrystals: synthesis, functional properties, and applications. Nanotechnol Sci Appl 8:45–54. https://doi.org/10.2147/NSA.S64386

Han J, Seo Y (2021) Comparison of cellulose dissolution behavior by alkaline and sulfuric acid solvents and their films' physical properties. Materials 14(18):1–9. https://doi.org/10.3390/ma14185273

Tabatabaei H, Ramin SM, Jafari HM, Nafchi AM, Dehnad D (2018) Preparation and characterization of nano-sio2 reinforced gelatin-k-carrageenan biocomposites. Int J Biol Macromol 111(May):1091–1099. https://doi.org/10.1016/j.ijbiomac.2018.01.116

Hasheminya SM, Mokarram RR, Ghanbarzadeh B, Hamishekar H, Kafil HS (2018) Physicochemical, mechanical, optical, microstructural and antimicrobial properties of novel kefiran-carboxymethyl cellulose biocomposite films as influenced by copper oxide nanoparticles (CuONPs). Food Packag Shelf Life 17(September):196–204. https://doi.org/10.1016/j.fpsl.2018.07.003

Hassannia-Kolaee M, Khodaiyan F, Pourahmad R, Shahabi-Ghahfarrokhi I (2016) Development of ecofriendly bionanocomposite: whey protein isolate/pullulan films with nano-SiO2. Int J Biol Macromol 86(May):139–144. https://doi.org/10.1016/j.ijbiomac.2016.01.032

He M, Zhao Y, Duan J, Wang Z, Chen Y, Zhang L (2014) Fast contact of solid-liquid interface created high strength multi-layered cellulose hydrogels with controllable size. ACS Appl Mater Interfaces 6(3):1872–1878. https://doi.org/10.1021/am404855q

Hu Y, Sheng J, Yan Z, Ke Q (2018) Completely amorphous cellulose biosynthesized in agitated culture at low temperature. Int J Biol Macromol 117:967–973. https://doi.org/10.1016/j.ijbiomac.2018.06.013

Huang K, Wang Y (2022) Recent applications of regenerated cellulose films and hydrogels in food packaging. Curr Opin Food Sci 43:7–17. https://doi.org/10.1016/j.cofs.2021.09.003

Jafarzadeh S, Alias AK, Ariffin F, Mahmud S (2017) Characterization of semolina protein film with incorporated zinc oxide nano rod intended for food packaging. Pol J Food Nutr Sci 67(3):183–190. https://doi.org/10.1515/pjfns-2016-0025

Jyothibasu JP, Kuo DW, Lee RH (2019) Flexible and free-standing electrodes based on polypyrrole/carbon nanotube/cellulose composites for supercapacitor application. Cellulose 26(7):4495–4513. https://doi.org/10.1007/s10570-019-02376-2

Kale RD, Alemayehu TG, Gorade VG (2020) Extraction and characterization of lignocellulosic fibers from Girardinia bullosa (Steudel) Wedd. (Ethiopian Kusha Plant). J Nat Fibers 17(6):906–920. https://doi.org/10.1080/15440478.2018.1539940

Kanai N, Honda T, Yoshihara N, Oyama T, Naito A, Ueda K, Kawamura I (2020) Structural characterization of cellulose nanofibers isolated from spent coffee grounds and their composite films with poly(vinyl alcohol): a new non-wood source. Cellulose 27(9):5017–5028. https://doi.org/10.1007/s10570-020-03113-w

Karunakaran G, Periyasamy AP, Tehrani A (2023) Extraction of micro, nanocrystalline cellulose and textile fibers from coffee waste. J Test Eval 51(5):20220487. https://doi.org/10.1520/jte20220487

Kilulya KF, Msagati TAM, Mamba BB, Catherine Ngila J, Bush T (2011) Chemical-grade cellulose in the determination of fatty acids using gas chromatography-mass. BioResources 6(3):3272–3288. https://doi.org/10.15376/biores.6.3.3272-3288

Klemm D, Heublein B, Fink H-P, Bohn A (2005) Cellulose: fascinating biopolymer and sustainable raw material. Angew Chem Int Ed 44(22):3358–3393. https://doi.org/10.1002/anie.200460587

Kumar A, Negi YS, Choudhary V, Bhardwaj NK (2020) Characterization of cellulose nanocrystals produced by acid-hydrolysis from sugarcane bagasse as agro-waste. J Mater Phys Chem 2(1):1–8. https://doi.org/10.12691/jmpc-2-1-1

Lim CJ, Arumugam M, Lim CK, Ee GCL (2020) Mercerizing extraction and physicochemical characterizations of lignocellulosic fiber from the leaf waste of Mikania Micrantha Kunth Ex H.B.K. J Nat Fibers 17(5):726–737. https://doi.org/10.1080/15440478.2018.1527742

Limousy L, Jeguirim M, Labaki M (2017) Energy applications of coffee processing by-products. Handbook of coffee processing by-products: sustainable applications. Elsevier. https://doi.org/10.1016/B978-0-12-811290-8.00011-6

Mohamed MA, Salleh WWN, Jaafar J, Ismail AF, AbdMutalib M, Sani NAA, Asri SEAM, Ong CS (2016) physicochemical characteristic of regenerated cellulose/N-doped TiO2 nanocomposite membrane fabricated from recycled newspaper with photocatalytic activity under UV and visible light irradiation. Chem Eng J 284(January):202–215. https://doi.org/10.1016/j.cej.2015.08.128

Mokhena TC, Sadiku ER, Mochane MJ, Ray SS, John MJ, Mtibe A (2021) Mechanical properties of cellulose nanofibril papers and their bionanocomposites: a review. Carbohydr Polym. https://doi.org/10.1016/j.carbpol.2021.118507

Najeeb MI, Sultan MTH, YoshitoAndou AUM, Shah KE, Jawaid M, Ariffin AH (2021) Characterization of lignocellulosic biomass from Malaysian's yankee pineapple AC6 toward composite application. J Nat Fibers 18(12):2006–2008. https://doi.org/10.1080/15440478.2019.1710655

Nam S, French AD, Condon BD, Concha M (2016) Segal crystallinity index revisited by the simulation of X-ray

diffraction patterns of cotton cellulose Iβ and cellulose II. Carbohyd Polym 135:1–9. https://doi.org/10.1016/j.carbpol.2015.08.035

Nomura S, Kugo Y, Erata T (2020) 13C NMR and XRD studies on the enhancement of cellulose II crystallinity with low concentration NaOH post-treatments. Cellulose 27(7):3553–3563. https://doi.org/10.1007/s10570-020-03036-6

Pagno CH, Costa TMH, De Menezes EW, Benvenutti EV, Hertz PF, Matte CR, Tosati JV, Monteiro AR, Rios AO, Flôres SH (2015) Development of active biofilms of quinoa (*Chenopodium quinoa* W.) starch containing gold nanoparticles and evaluation of antimicrobial activity. Food Chem 173(April):755–762. https://doi.org/10.1016/j.foodchem.2014.10.068

Pang JH, Liu X, Miao Wu, Yu Ying Wu, Zhang XM, Sun RC (2014) Fabrication and characterization of regenerated cellulose films using different ionic liquids. J Spectrosc 2014:8. https://doi.org/10.1155/2014/214057

Rizwan M, Gilani SR, Durrani AI, Naseem S (2021) Cellulose extraction of alstonia scholaris: a comparative study on efficiency of different bleaching reagents for its isolation and characterization. Int J Biol Macromol 191(April):964–972. https://doi.org/10.1016/j.ijbiomac.2021.09.155

Rodríguez Valencia N, Franco DZ (2010) Los Subproductos Del Café: Fuente de Energía Renovable. Avances Técnicos Cenicafé. ISSN-0120-0178

Segal L, Creely JJ, Martin AE, Conrad CM (1959) An empirical method for estimating the degree of crystallinity of native cellulose using the X-ray diffractometer. Text Res J 29(10):786–794. https://doi.org/10.1177/004051755902901003

Seidi F, Yazdi MK, Jouyandeh M, Habibzadeh S, Munir MT, Vahabi H, Bagheri B, Rabiee N, Zarrintaj P, Saeb MR (2022) Crystalline polysaccharides: a review. Carbohydr Polym 275(1):118624. https://doi.org/10.1016/j.carbpol.2021.118624

Setiawan JV, Adhitama R, Goeltom MT, Askitosari TD, Yang DC, Sukweenadhi J (2022) The potential of rice bran waste (*Oryza sativa* L.) and shrimp shell waste as chitin nanowhisker with glycerol plasticizer in the production of bioplastic. In: IOP conference series: earth and environmental science, vol 1083, p 012045. Institute of Physics. https://doi.org/10.1088/1755-1315/1083/1/012045.

Shi C, Chen Y, Yu Z, Li S, Chan H, Sun S, Chen G, He M, Tian J (2021) Sustainable and superhydrophobic spent coffee ground-derived holocellulose nanofibers foam for continuous oil/water separation. Sustain Mater Technol 28:e00277. https://doi.org/10.1016/j.susmat.2021.e00277

Shin E, Choi S, Lee J (2018) Fabrication of regenerated cellulose nanoparticles/waterborne polyurethane nanocomposites. J Appl Polym Sci 135(35):1–8. https://doi.org/10.1002/app.46633

Silverstein RM, Webster FX, Kiemle DJ (2005) Spectrometric identification of organic compounds, 7th edn. Wiley, New York. https://doi.org/10.1016/0022-2860(76)87024-X

Sirviö JA (2019) Fabrication of regenerated cellulose nanoparticles by mechanical disintegration of cellulose after dissolution and regeneration from a deep eutectic solvent. J Mater Chem A 7(2):755–763. https://doi.org/10.1039/c8ta09959f

Tu Hu, Zhu M, Duan Bo, Zhang L (2021) Recent progress in high-strength and robust regenerated cellulose materials. Adv Mater 33(28):1–22. https://doi.org/10.1002/adma.202000682

Wang B, Nie Yi, Kang Z, Liu X (2022) Effects of coagulating conditions on the crystallinity, orientation and mechanical properties of regenerated cellulose fibers. Int J Biol Macromol 225:1374–1383. https://doi.org/10.1016/j.ijbiomac.2022.11.195

Wang S, Ang Lu, Zhang L (2016) Recent advances in regenerated cellulose materials. Prog Polym Sci 53:169–206. https://doi.org/10.1016/j.progpolymsci.2015.07.003

Xiong X, Duan J, Zou W, He X, Zheng W (2010) A PH-sensitive regenerated cellulose membrane. J Membr Sci 363(1–2):96–102. https://doi.org/10.1016/j.memsci.2010.07.031

Zeleke NM, Sinha DK, Mengesha GA (2022) Chemical composition and extraction of micro crystalline cellulose from outer skin isolated coffee husk. Adv Mater Sci Eng 2022:13. https://doi.org/10.1155/2022/7163359

Zhang LQ, Niu B, Yang SG, Huang HD, Zhong GJ, Li ZM (2016) Simultaneous preparation and dispersion of regenerated cellulose nanoparticles using a facile protocol of dissolution-gelation-isolation-melt extrusion. ACS Sustain Chem Eng 4(5):2470–2478. https://doi.org/10.1021/acssuschemeng.5b01171

Zhang X, Zhu J, Liu X (2012) Preparation and characterization of regenerated cellulose blend films containing high amount of poly(vinyl alcohol) (PVA) in ionic liquid. Macromol Res 20(7):703–708. https://doi.org/10.1007/s13233-012-0106-2

Zhu Q, Wang J, Sun J, Wang Q (2020) Preparation, characterization, and oxygen barrier properties of regenerated cellulose/polyvinyl alcohol blend films. BioResources 15(2):2735–2746. https://doi.org/10.15376/biores.15.2.2735-2746